Pion-nucleus spin-flip strength at low and resonance energies

B. G. Ofenloch,* R. A. Giannelli, and B. G. Ritchie
Arizona State University, Tempe, Arizona 85287-1504

J. M. O'Donnell,† J. N. Knudson, and C. L. Morris
Los Alamos National Laboratory, Los Alamos, New Mexico 87545

C. M. Kormanyos,‡ A. Saunders, and J. Z. Williams§
Nuclear Physics Laboratory, University of Colorado, Boulder, Colorado 80309-0446

R. A. Lindgren
University of Virginia, Charlottesville, Virginia 22904

B. L. Clausen
Geoscience Research Institute, Loma Linda University, Loma Linda, California 92350
and Physics Department, La Sierra University, Riverside, California 92515
(Received 13 September 1996)

Cross sections have been measured for 65 MeV π^+ scattering to the ^{10}B ground and first four excited states. The 1.74 MeV excited state results provide the first measurement of the energy dependence of the isovector spin-flip strength parameter. Our analysis indicates that the observed empirical enhancement of the isovector spin-flip strength has little or no dependence on energy at and below resonance. A mass dependence for the empirical enhancement factor may exist. [S0556-2813(97)03703-5]

PACS number(s): 25.80.Ek, 21.30.Fe, 27.20.+n

I. INTRODUCTION

A useful approach to providing a clearer description of the pion-nucleus reaction mechanism is to identify and study transitions of relatively simple structure. With data for such transitions, models of the reaction mechanism can be stringently tested. One insightful representation of the pion-nucleus reaction mechanism is that proposed by Carr *et al.* [1]. In this model, the spin-dependent portion of the effective pion-nucleus interaction for unnatural parity transitions, is characterized by a single isospin- and energy-dependent strength parameter t^{LS}. The parametrization of the pion-nucleus potential in this approach contains couplings to spin-orbit, spin-current, central, and Δ-hole components:

$$U_{\pi A}=t^{LS}\rho_J^s+\frac{dt^{LS}}{dE}\rho_J^{\prime s}+\frac{dt^C}{dE}\rho_J^{\prime}+t_{\pi\Delta}\rho_J^{\Delta}. \qquad (1)$$

A judicious choice of states to be studied can simplify tests of this potential by isolating or eliminating one or more of the terms given in Eq. (1). For instance, with ''stretched'' transitions, the effects of the spin-orbit and spin-current terms can be isolated, since the central component vanishes as the current density is equal to zero for such transitions [1]. If low energy pions far from resonance are used, the contributions from the Δ-hole component for isovector transitions are minimal, and if high spin transitions are used, those same Δ-hole admixtures in isovector states are negligible [2]. The spin-current term, usually ignored, would be small at low energies since dt^{LS}/dE is expected to be small [1].

From this discussion, then, it is seen that the spin-flip strength t^{LS} can be isolated by obtaining cross sections for low energy pion excitation of unnatural parity stretched states. Such measurements provide an *empirical* determination of the spin-flip strength for the scattering potential. On the other hand, the strength parameter of the spin-orbit portion of the scattering potential can also be *predicted* by examining the p-wave portion of the spin-orbit operator of the pion-nucleon interaction, basing those predictions on pion-nucleon phase shifts [3,4]. A test of the performance of the approach of Ref. [1] would be possible by comparing empirical and predicted values.

While the experimental conditions are restrictive, suitable experiments for determining the isovector portion of the strength parameter can be performed. In this work, we report the results of 65 MeV π^+ scattering to a number of states, but particularly the 1.740 MeV ($J^\pi=0^+;T=1$) excited state of ^{10}B. Excitation of this state provides a stretched, unnatural parity, pure $M3$, and spin-flip and isospin-flip transition. All of the low-lying excitations of ^{10}B have reliably measured energies so that the precise locations of those states are known [5]. With acceptable energy resolution, cross sections for these states can be measured and, with the data from the 1.74 MeV state, an empirical determination of t_1^{LS} (where the subscript 1 indicates an isovector transition) can be made.

*Present address: Texas Instruments, P.O. Box 405, MS/3484, Lewisville, TX 75067.

†Present address: Dept. of Physics, University of Minnesota, Minneapolis, MN 55455.

‡Present address: Payerstrasse 49, 72764 Reutlingen, Germany.

§Present address: Arete Associates, 1725 Jefferson Davis Highway, Suite 703, Arlington, VA 22202.

By using the data reported here coupled with inelastic pion scattering data obtained at resonance energies for this transition [6], as well as data collected for other stretched transitions in other nuclei as detailed below, an indication of the energy dependence of this isovector strength parameter can be obtained. This same analysis is also extended to isoscalar stretched transitions by analyzing previously published data on those transitions in the same framework.

II. EXPERIMENTAL METHOD

The experiment was performed using the Low Energy Pion (LEP) channel [7] at the Clinton P. Anderson Meson Physics Facility. The experimental apparatus used within the channel included the SCRUNCHER and the Clamshell spectrometer. The SCRUNCHER is a superconducting radio frequency cavity coupled to the accelerator radio frequency signal such that the electric fields within the cavity compress the pion beam momentum spread; the device is described in detail elsewhere [8–10]. The principal feature of the Clamshell spectrometer is a varying width dipole magnet, providing a smoothly varying, easily determined acceptance as a function of scattered pion momentum; characteristics and the operation of the spectrometer is described in detail elsewhere [11,12]. By using the unique characteristics of these devices, an enhanced pion flux with minimized energy spread was obtained, which improved the overall energy resolution for the scattered pions to a level sufficient to separate the states of interest, as detailed below.

The incident π^+ kinetic energy was 65 MeV for all data reported here. The momentum spread selected for the channel was 2%, yielding a pion flux of about 10^7 s^{-1} for full production beam current. The SCRUNCHER was located in the LEP cave following the last quadrupole of the LEP channel, and operation with that device reduced the contribution of the channel momentum spread to the scattered pion energy resolution obtained by about a factor of 4–5.

To achieve measurable cross sections for the transition of interest, measurements at large scattering angles were required. Data were obtained at laboratory scattering angles of 65°, 80°, and 100°, the latter being the maximum angle possible for the Clamshell spectrometer with the SCRUNCHER in place. Spectrometer acceptance measurements showed a smooth uniform increase of acceptance with decreasing scattered pion momentum as measured previously [11,12]. Utilizing the capabilities of the SCRUNCHER and Clamshell, the overall energy resolutions obtained varied from 390 keV at 65° to 490 keV at 100°.

Data were obtained for targets of sintered graphite and isotopically enriched ^{10}B and ^{11}B. The sintered ^{10}B target was 107 mg/cm^2 in thickness and composed of 92% ^{10}B and 8% ^{11}B. The binder used in the sintering process left a small residue of nitrogen which provided an inconsequential contribution to the background of the final spectra. The pure ^{11}B target was 128 mg/cm^2 in thickness and was used for removing the contributions of the ^{11}B content of the ^{10}B target by subtracting spectra, normalized for thickness and pion flux, obtained for the ^{11}B target at the three spectrometer angles.

A graphite target 131 mg/cm^2 in thickness was used for energy calibration, absolute normalization, and determining a scattered pion line shape for the spectrometer. The elastic and first excited states of ^{12}C, which dominated the graphite spectrum, have energies which bracket the missing mass region of interest in ^{10}B, providing an accurate energy calibration for the scattered pions detected with the spectrometer. To obtain an absolute cross section normalization, carbon data obtained here were normalized to the previously measured [13] elastic cross sections at 65 MeV.

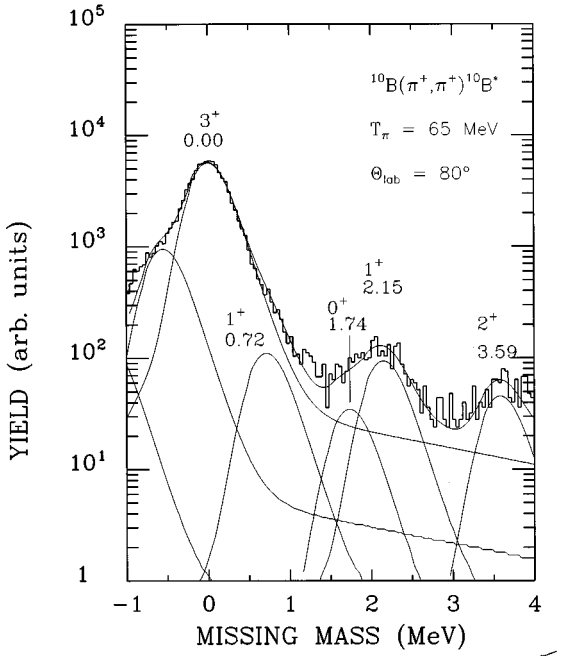

FIG. 1. ^{10}B spectrum below 4 MeV in missing mass energy obtained after subtraction of ^{11}B content. The laboratory scattering angle is 80°. Excitations of interest in ^{10}B are labeled by spin, parity, and energy. Also shown is the result of the peak fitting procedure described in the text.

The line shape used to fit the ^{10}B spectra for each scattering angle was obtained by fitting the elastic peak observed in the spectra of the carbon target for each scattering angle (using the program NEWFIT [14]). The graphite target was ideal for this purpose since ^{12}C has nearly the same charge, density, and thickness as the ^{10}B target used, and has clearly separated ground state and first excited state peaks. To accomodate the slight differences in thickness between the three different targets, *only the elastic peak width was varied* in the fits to the boron spectra; all other parameters were fixed to the carbon line shape for each angle.

All ^{10}B spectra were fit with peaks *fixed* to the known energies [5] for excitations of ^{10}B in the energy range 0.0 to 7.0 MeV, though we only report data here for states below 4 MeV. The spectrum obtained at 80° for ^{10}B after the subtraction of the ^{11}B content is shown in Fig. 1. Also shown is a typical fit to such a spectrum. No backgrounds were found in the carbon spectrum for each angle, so no background was assumed for energies above the ground state. Some background around 4 MeV is observed in the ^{10}B spectra and is most likely a combination of the 5.11 MeV (2^-;0) and 4.92 MeV (0^-;0) excited states of ^{14}N. Below the ground state, nitrogen and aluminum ground states can be seen, the latter most likely due to some scattering of the tails of the pion beam particle distribution from target chamber materials. No

TABLE I. Center of mass differential cross sections measured in this work for 65 MeV π^+ scattering from levels in ^{10}B, in μb/sr. Uncertainties indicated include statistical and normalization uncertainties.

Energy level (MeV)	$d\sigma/d\Omega\|_{\text{c.m.}}$ (μb/sr) $\theta_{\text{lab}}=65°$	$\theta_{\text{lab}}=80°$	$\theta_{\text{lab}}=100°$
0.0	1060±120	1470±90	2500±400
0.718	19±2	29±2	93±16
1.740	4±1	9±1	14±3
2.154	14±2	25±2	38±6
3.587	5±1	12±1	29±5

other strength is observed in the region below 4 MeV other than ^{10}B excitations. The cross sections obtained are given in Table I.

Cross sections for the 1.74 MeV state are small due to the large momentum transfer required and, with the experimental energy resolution obtained, this peak somewhat overlaps the 2.154 MeV state. Nonetheless, the peak is visible in Fig. 1 as a knee on the low energy side of the 2.154 MeV state, and cross sections for that peak can be extracted due to the precise knowledge of the locations of the low-lying states in ^{10}B. To buttress confidence in the peak area extracted for the ^{10}B $(0^+;1)$ state, its statistical significance was verified by examining changes in the fit χ^2 for the region surrounding the state when the fit was modified. Removal of the 1.74 MeV peak from the fit caused the χ^2 to change by a factor of 2 within the region 0.5 and 3.0 MeV. If the 0.718 and 2.154 MeV states were allowed to vary in energy from their accurately known positions (to 0.93 and 2.10, respectively), without inclusion of the 1.74 MeV state, the χ^2 resulting from such a grossly distorted fit was inferior to the fit including the 1.74 MeV state.

III. THEORETICAL ANALYSIS

A. Overview of analysis method

In this section, we describe how the enhancements of the spin-flip strength as compared to the predictions for those parameters based on pion-nucleon phase shifts were determined empirically by using the cross sections measured here and in previous studies. By following the procedure outlined in this section, an empirical determination of the isovector spin-flip transition strength, using the normalization factor found for the pure $M3$ 1.74 MeV transition, was made for 65 MeV pions. A similar analysis was then conducted at resonance energies for data published previously on both isoscalar and isovector stretched transitions in ^{10}B as well as other nuclei. These analyses are discussed in turn in the following sections.

The common theoretical framework for our analysis was the MSU potential [17], and our approach was similar to that used by Clausen *et al.* [18,19]. Following that approach, the differential cross section for a particular pion scattering transition for a specific multipolarity was given by

$$\frac{d\sigma}{d\Omega}=N_{\Sigma\Lambda}\times f^2_{\text{c.m.}}\times(M_1)^2\times\left(\frac{M_0}{M_1}Z_0+Z_1\right)^2,$$

where $N_{\Sigma\Lambda}$ is an empirical normalization factor determined for a particular multipole, $(M_\tau)^2$ is the pure isoscalar or isovector cross section calculated using the distorted wave impulse approximation (DWIA), and the Z_τ are spectroscopic factors. $f^2_{\text{c.m.}}$ is a center-of-mass correction factor given by

$$f^2_{\text{c.m.}}=\left(\frac{A}{A-1}\right)^L,$$

where A is the atomic mass of the nucleus and L is the angular momentum transfer in the reaction. The spectroscopic factors are directly related to the reduced transition probabilities. Pion-nucleon phase shift results were used to generate the spin-flip strength parameters of equation 1 for the DWIA calculations, so that the deduced normalization factors provided an empirical measure of the enhancement of that strength.

Comparisons of the predicted cross sections using these normalizations was made to the other states within a given nucleus which have mixtures of these multipolarities to determine empirical values of the spectroscopic factors so that reduced transition probabilities could be inferred for those states. The resulting probabilities were compared with previous work from pion scattering and other probes. The general agreement found from these comparisons provided confidence for this approach, as detailed below.

For the ^{10}B transitions of interest here, the multipoles involved are $E2$, $M3$, or admixtures of these multipoles. In order to calculate cross sections, then, it was necessary to determine the normalization factor $N_{\Sigma\Lambda}$ for each of these multipolarities.

For $M3$ transitions, the spectroscopic factor Z_1 was first determined by finding the value of Z_1 needed to force the calculations using the MSU potential to reproduce the reduced transition probability $B(M3)$ for the 1.74 MeV, pure $M3$, isovector transition. As noted below, this transition probability has been deduced in other studies, and the previously published value is used as input here to determine the spectroscopic factor Z_1. The transition density calculated using this spectroscopic factor was then used to generate DWIA predictions for the cross sections. The normalization factor for $M3$ transitions N_{M3} was then deduced as the factor needed to obtain agreement between the DWIA predictions and the cross sections measured here for this 1.74 MeV transition; this same factor was used to normalize all predictions with $M3$ character.

Next, the procedure was repeated using the 0.718 MeV transition in ^{10}B in order to find the normalization factor N_{E2} appropriate for $E2$ transitions. For the 0.718 MeV transition, the $E2$ multipole dominates the transition. The tran-

TABLE II. Values of the MSU potential parameters obtained at 65 and 162 MeV using the procedure described in the text. The parameters at 50 MeV are supplied for comparison. The parameters b_1 and c_1 were not determined at 65 MeV as $N=Z$ for the ^{10}B nucleus.

MSU potential parameters	Parameter set E 50 MeV [17]	χ^2 minimized parameters at 65 MeV	χ^2 minimized parameters at 162 MeV	Previously determined at 162 MeV [15,16,18]
b_0 fm	$-0.061, 0.006i$	$-0.055, 0.0002i$	$-0.083, 0.029i$	$-0.083, 0.029i$
b_1 fm	$-0.130, -0.002i$	$-0.130, -0.002i$	$-0.125, 0.003i$	$-0.125, 0.003i$
c_0 fm^3	$0.700, 0.028i$	$0.530, 0.358i$	$0.265, 0.500i$	$0.450, 0.670i$
c_1 fm^3	$0.460, 0.013i$	$0.460, 0.013i$	$0.385, 1.550i$	$0.240, 0.330i$
B_0 fm^4	$-0.020, 0.110i$	$-0.085, 0.072i$	$-0.200, 0.080i$	$-0.150, 0.280i$
C_0 fm^6	$0.0, 0.0i$	$0.0, 0.0i$	$0.0, 0.0i$	$0.0, 0.0i$
C_2 fm^6	$0.360, 0.540i$	$0.183, 0.717i$	$0.400, 6.500i$	$1.290, 2.95i$
λ	1.400	1.615	1.000	1.000

sition is isoscalar, and, thus, the spectroscopic factor determined was Z_0. The reduced transition probability $B(E2)$ for this transition has also been determined in other studies as discussed below, so the calculations were forced to reproduce this $B(E2)$. Then, as before, the normalization factor N_{E2} was determined by ascertaining the factor needed to obtain agreement between the cross sections measured here and the DWIA predictions for the transition. (In this case, however, subsequently adding some $M3$ contribution improved the predictions for the largest scattering angle as deduced elsewhere (for instance, Ref. [6]).

To deduce any energy or mass dependence for any enhancement deduced for the strength parameters, we extended our analysis to data taken for ^{10}B at resonance and to stretched transitions in other nuclei. The spectroscopic factors Z_τ for transitions in nuclei other than ^{10}B were taken from published studies, either using the published values for the Z_τ or from forcing agreement with published reduced transition probabilities to deduce the spectroscopic factors. (In the MSU formalism, proton, electron, and pion scattering are related through a common spin transition density when examining stretched transitions, so data from probes other than the pion may be used.) These spectroscopic factors were then used to deduce the normalizations required to make the predicted DWIA cross sections agree with the experimental data for those nuclei, and, in turn, generated empirical estimates for the enhancements of the spin-flip strengths for those nuclei.

Calculated cross sections were generated using the computer codes ALLWRLD [15] and MSUDWPI [16]. Both codes used the MSU potential [17] to generate the calculated cross sections. The ALLWRLD code was used to generate the transition densities for input to the DWIA pion scattering code MSUDWPI, which in turn was used to generate the differential cross sections. At each energy, the MSU potential parameters were determined by fitting the predictions of this potential to previously published carbon elastic differential cross sections at each energy. Carbon was used because of its similar charge and, as noted below, data exists at 65 MeV and at resonance. Matter densities for nuclei were generally taken from published elastic scattering densities, though in few cases some modifications were made as noted below.

B. Analysis of 65 MeV data

We now discuss how the measurements reported here were used to estimate the isovector spin-flip strength at 65 MeV. Though we will use the procedure discussed in the previous section, we emphasize that *the MSU potential parameters, matter densities, and fundamental E2 and M3 spectroscopic factors were determined by data independent of the pion data measured in this work.*

Parameters for the MSU potential at 65 MeV have not been previously determined, so the parameters were obtained by performing a χ^2 minimization of the cross section predictions made with the MSU potential to the measured angular distribution of Blecher *et al.* [13] for elastically scattered π^+ on ^{12}C. In performing the χ^2 minimization, the MSU potential parameters were generally constrained to have values between previously determined values at 50 MeV [17] and 162 MeV [15,16]. The value of λ, however, was not constrained as analyses have shown that it could have values larger than the value found previously at 50 MeV [20].

The previously determined values for the potential parameters resulted from global fits of pion-nucleus scattering data with a database for targets from carbon to lead. It is thus not surprising that refinement of the parameters would result in a much better description of the existing carbon data than would those resulting from the global fit. The MSU potential parameters obtained in this fitting process to the carbon elastic data are given in Table II, and the good agreement between the predictions of the potential and the Blecher *et al.* data is shown in Fig. 2. Also included in the table, for comparison, are the previously published parameters [17] obtained at 50 MeV. The values obtained are generally seen to either be close to the previously determined 50 MeV parameters or between the 50 MeV values and those determined previously for 162 MeV. This comparison provides support that the parameters determined are reasonable.

Turning attention to ^{10}B, a quadrupole contribution to the elastic scattering cross sections for ^{10}B had been observed previously to be of some importance in measurements made at resonance energies [6]. However, at 65 MeV, the same formalism used in Ref. [6] indicates that this contribution is smaller than our experimental uncertainties. Thus, this contribution was ignored for the 65 MeV analysis. The harmonic

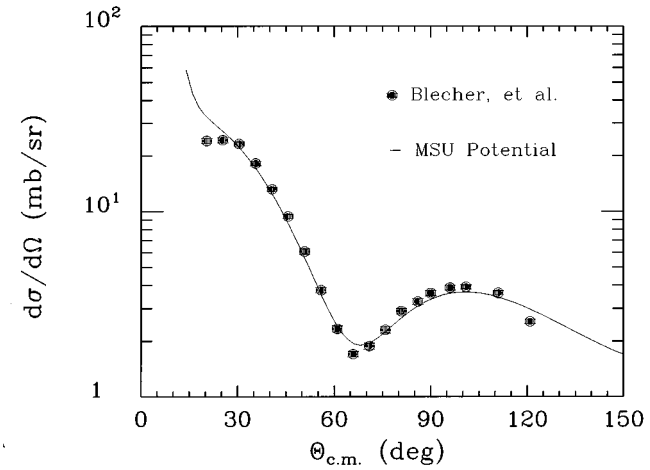

FIG. 2. Comparisons of the predictions of the MSU potential using the parameters given in Table II and the differential cross sections for elastically scattered 65 MeV π^+ measured by Blecher *et al.* [13].

Gaussian matter density distribution and harmonic oscillator wave function parameters for ^{10}B were obtained from published values [21].

The isoscalar and isovector spectroscopic factors Z_0 and Z_1 used in our analysis as initial values for subsequent fits were inferred from published experimental [5,22,23] and theoretical [23] values of the reduced transition probabilities for the first four excited states of ^{10}B. Electron scattering data for the 1.74 MeV pure $M3$ transition in ^{10}B [22,26] provided an experimental value of the reduced transition probability $B(M3)$. Existing proton scattering data provided an empirical determination of the reduced transition probability $B(E2)$ for the $E2$ portion of the 0.718 MeV transition [23]. By performing the analysis in this manner, the quadrupole enhancements of the $E2$ portions [6,24] of the transitions under consideration would be empirically incorporated in the calculations. (If one were to consider the effects of core polarization, as in a previous study using resonance energy pions [25], no enhancements would be necessary. This approach, however, was not used in this analysis as it was desired to present the results according to standard practices.)

The reduced transition probability used to obtain the spectroscopic factor for the pure $M3$ transition to the 1.740 MeV $(0^+;1)$ excited state was $8.2\pm2.0e^2$ fm^6, a corrected value [26] obtained from the original experiment [22]. This value is consistent with the reduced transition probability of $9.5\pm0.12e^2$ fm^6 determined experimentally using resonance energy pions [6]. The well-known reduced transition probability determined from the radiative width of the $(1^+;0)\rightarrow(3^+;0)$ transition was used to obtain the Z_0 spectroscopic amplitude for the $E2$ portion of the 0.718 MeV excitation [5].

The predicted value of the reduced transition probability for the pure $M3$ transition at 1.74 MeV was computed using ALLWRLD. Since the $B(M3)$ value is scaled by the Z_1 spectroscopic factor ($Z_0=0$), the factor was chosen such that the computed $B(M3)$ value would be the same as the empirically determined value. This value of Z_1 also scales the transition densities computed by ALLWRLD, which are used as input to MSUDWPI. The cross sections computed by MSUDWPI were then fit to the data using a χ^2 minimization procedure. These predicted cross section fits were then scaled by the normalization factor N_{M3}. The normalization factor N_{M3} obtained in this manner was used for all $M3$ portions of transitions studied. Subsequent normalizations of the $M3$ portions of the other transitions gave inferred values for the spectroscopic coefficients for those transitions and, thus, the reduced transition probabilities.

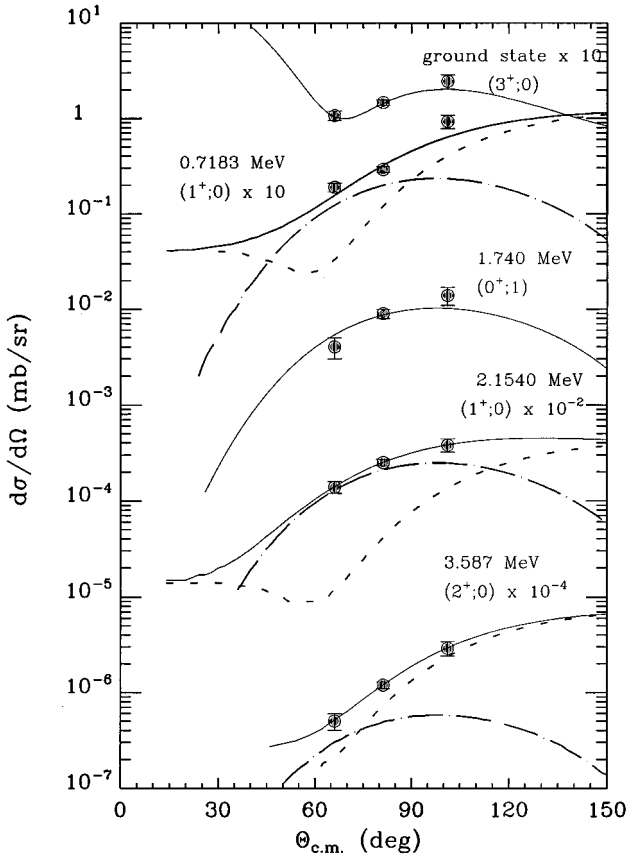

FIG. 3. Comparisons of differential cross sections obtained here for the elastic and first four excited states of ^{10}B to predictions made using the procedure discussed in the text. Error bars indicate statistical uncertainties in the measured cross sections. The dashed (dot-dashed) curves represent $E2$ ($M3$) contributions to the summed cross section predictions; the sums are indicated by the solid lines.

The normalization of the $E2$ portion of the 0.718 MeV transition was found in a similar manner. Using a Z_0 value so that the $B(E2)$ value computed by ALLWRLD was identical to the empirically determined value, the predicted cross sections were fit to the data. The resulting fit assumed that the predicted cross sections were composed of $E2$ and $M3$ portions. A normalization for each portion was then determined. The $E2$ normalization value was noted and used in determining the predicted cross sections of the 2.154 and 3.587 MeV transitions. The isoscalar spectroscopic factor Z_0 for the $M3$ portion of the transition was then adjusted so that its product with the normalization factor N_{M3} gave the normalization found for the $M3$ portion of the 0.718 MeV transition during the χ^2 minimization fit to the data for that state. This

TABLE III. Reduced $E2$ transition probabilities determined in this work for transitions in ^{10}B. The $E2$ value for the 0.718 MeV state has been set to the accepted value [5]. The third column indicates the accepted values for these transitions [5]. The final column provides the experimental values at resonance energies for comparison from Ref. [6].

	$B(E2\uparrow)$ (e^2 fm^4)		
Excited state ($J^\pi;T$)	This work	Accepted value	π^+ at 162 MeV
0.718 MeV ($1^+;0$)	1.808	1.81 ± 0.03	0.92 ± 0.15
1.740 MeV ($0^+;1$)	-	-	-
2.154 MeV ($1^+;0$)	0.63 ± 0.02	0.70 ± 0.08	0.46 ± 0.12
3.587 MeV ($2^+;0$)	1.13 ± 0.03	0.87 ± 0.25	0.67 ± 0.12

Z_0 thus yielded a determination of the reduced transition probability $B(M3)$ for the $M3$ portion of this transition.

The first three nonstretched transitions of ^{10}B were assumed to be mainly composed of $E2$ and $M3$ portions. The normalizations N_{E2} and N_{M3} obtained as described above were used in determining the Z_0 spectroscopic amplitudes for the $E2$ and $M3$ portions of the 2.154 and 3.587 MeV states by performing a χ^2 minimization of the predicted cross sections to the data assuming the transitions were composed of $E2$ and $M3$ portions. Values for the reduced transition probabilities $B(E2)$ and $B(M3)$ of these transitions were thereby obtained.

Normalizations for the $E2$ and $M3$ contributions of the cross section predictions were determined to be 0.53 ± 0.06 and 1.83 ± 0.22, respectively, with the normalization uncertainties generated from average values of the individual uncertainties. The results of the calculations based on these normalizations are illustrated in Fig. 3. The shapes and magnitudes of the measured angular distributions are described quite well with these calculations.

The empirical $E2$ reduced transition probabilities $B(E2)$ inferred from these calculated angular distributions are given in Table III. The inferred $B(E2)$ values for the 2.154 and 3.587 MeV states agree with the accepted values [5], though the value obtained here for the 3.587 MeV state is just within the uncertainty in the accepted value [5]. Reduced transition probabilities obtained using resonance energy pions [6] are also given in Table III. The $B(E2)$ values previously inferred at resonance are both lower than the values determined in this work and in poorer agreement with the accepted values.

The empirical $M3$ reduced transition probabilities $B(M3)$ determined here for states in ^{10}B are given in Table IV. These empirical results can be compared to predictions by Lewis *et al.* [23]. In some cases, the empirical $B(M3)$ values deduced here indicate a preference for the predictions for one of the potentials used in Ref. [23]. For instance, the empirical $B(M3)$ for the 0.718 MeV state is comparable to the value obtained from the Cohen-Kurath (8-16) potential, while the $B(M3)$ for the 3.587 MeV ($2^+;0$) state agrees with the Barker set I and III values. The $B(M3)$ value obtained for the 2.154 ($1^+;0$) state does not agree with the results of any of the sets of values but would seem to prefer the lower values from the Barker set I and III potential, whereas the previously determined experimental value at resonance [6] was indistinguishable for the results using the Cohen-Kurath or Barker potentials. Generally speaking, no clear preference for one potential is exhibited by the data obtained here, though the lower states agree better with the Cohen-Kurath (8-16) potential while the higher states are more in agreement with Barker set 3.

Overall, the agreement with previous work and the agreement illustrated in Fig. 3 provides confidence that the approach outlined in the previous section is valid. With these reduced transition probabilities in hand, the empirical isovector spin-flip strength parameter at 65 MeV was obtained in the same manner as in a previous study [1]. The strength parameter S_i is related to the t^{LS} parameter in Eq. (1) by the relation

$$t_i^{LS}=\frac{2\pi\hbar^2}{\omega_c}S_i\,,$$

where ω_c is the reduced energy in the pion-nucleus center of mass frame and the subscript i refers to either the isoscalar ($i=0$) or isovector ($i=1$) portion. For the data obtained

TABLE IV. Reduced $M3$ transition probabilities determined in this work for transitions in ^{10}B. The $B(M3)$ value for the 1.740 MeV state is set to the value obtained from electron scattering [22,26]. The third column provides the experimental values for the same states in ^{10}B from Zeidman *et al.* [6] at 162 MeV for comparison. The last columns give theoretical values from Lewis *et al.* [23] based on the Cohen-Kurath (8-16) potential, Barker set 1, and Barker set 3 predictions, denoted as CK, B-1, and B-3, respectively.

Energy of state	Experimental $B(M3\uparrow)$		Theoretical $B(M3\uparrow)$		
($J^\pi;T$) (MeV)	This work (e^2 fm^6)	π^+ at 162 MeV[b] (e^2 fm^6)	CK (e^2 fm^6)	B-1 (e^2 fm^6)	B-3 (e^2 fm^6)
0.718 ($1^+;0$)	0.15 ± 0.01	0.42 ± 0.16	0.13	0.33	0.31
1.740 ($0^+;1$)	8.2	9.5 ± 0.12	7.47	7.76	7.17
2.154 ($1^+;0$)	0.17 ± 0.02	0.43 ± 0.12	0.50	0.37	0.34
3.587 ($2^+;0$)	0.04 ± 0.01	-	0.01	0.03	0.04

here at 65 MeV, the isovector spin-flip strength parameter was found to be 0.10 ± 0.02 fm^6. The uncertainty in the empirical value obtained for this quantity results from the uncertainties in the experimentally determined reduced transition probability and differential cross sections.

For comparing this empirically deduced strength parameter to phase shifts, the spin-orbit parameters for the calculation of the reduced radial transition potential were determined using the pion-nucleon phase shifts of Arndt and Roper [3]. The mean square target independent strength parameter $|S_1|^2$ derived from pion-nucleon phase shifts was found to be 0.056 fm^6, whereas the empirical value obtained in this work, as noted above, is 0.10 ± 0.02 fm^6. Thus, *the empirical value for the isovector spin-flip strength parameter is enhanced over the phase shift value by a factor of 1.8 $\pm$ 0.4 at 65 MeV.*

C. Analysis of resonance energy data

Published data obtained at resonance for stretched transitions in ^{10}B, ^{16}O, ^{14}C, ^{28}Si, ^{26}Mg, ^{54}Fe, and ^{60}Ni [6,18,19,27–30] can also be analyzed in this framework. (Data for ^{14}C and ^{16}O were measured at 164 MeV. All other data were measured at, and all calculations were performed for, 162 MeV.) MSU potential parameters were obtained for 162 MeV in the same manner as at 65 MeV by performing a χ^2 minimization of the potential predictions to published ^{12}C elastic scattering data [31]; those parameters are given in Table II. Comparison of the MSU potential parameters obtained here for 162 MeV incident pions to previously determined values using a different set of data show that the imaginary portion of the C_2 absorption parameter is roughly twice those values while the s- and p-wave scattering parameters b_0 and c_0 are very nearly the same [15,16,18]. The differences which can be noted in Table II between the best fit obtained here for ^{12}C and the global fit to data for ^{14}C, ^{28}Si, ^{54}Fe, and ^{60}Ni nuclei obtained in Ref. [18] are typical of the variations in the parameters needed to fit data for a particular nucleus (in this case ^{12}C) in a fashion superior to that provided by the parameters of a global fit.

As the isovector s- and p-wave MSU potential parameters do not enter into the calculations for $N=Z$ nuclei [for $N=Z$, $\delta\rho(r)$ is assumed to be 0], those parameters could not be determined with elastic scattering data for ^{12}C. Hence, ^{13}C elastic scattering data were used to determine b_1 and c_1 [32]. An optimal fit to the ^{13}C data was found using the value for b_1 given in Ref. [18] and using $c_1 = (0.385, 1.55i)$ fm^3. Though this c_1 value is larger than the previous value used, $c_1 = (0.19, 0.35i)$ fm^3, very similar predictions are obtained with the larger value, as well as improved fits to the data obtained for ^{14}C and ^{54}Fe. The resulting fits are comparable in quality to the results at 65 MeV shown in Fig. 2.

Further optimizations of the fits for ^{10}B, ^{16}O, and ^{28}Si solely involved varying the radius and second parameters (α) of the harmonic Gaussian matter density distributions in order to obtain an optimal χ^2 fit to the published elastic scattering data [6,33,34]. The radius and second parameters (r,w) obtained for ^{10}B, ^{16}O, and ^{28}Si were (1.77 fm, 0.45 fm), (1.78 fm, 1.04 fm), and (2.09 fm, 2.24 fm), respectively. The nickel, magnesium, and iron densities were two-parameter Fermi distributions with parameters given in previous analyses [18,19,30]. The spectroscopic amplitudes and shell model levels used in the analysis of ^{16}O and ^{28}Si were those given in a previous analysis [1]. The parameters for the other nuclei were taken from Refs. [18,19,21,30]. In a similar manner to that described for 65 MeV, the isoscalar and isovector strength parameters at 162 MeV were obtained, and those are illustrated in Figs. 4(a) and 4(b).

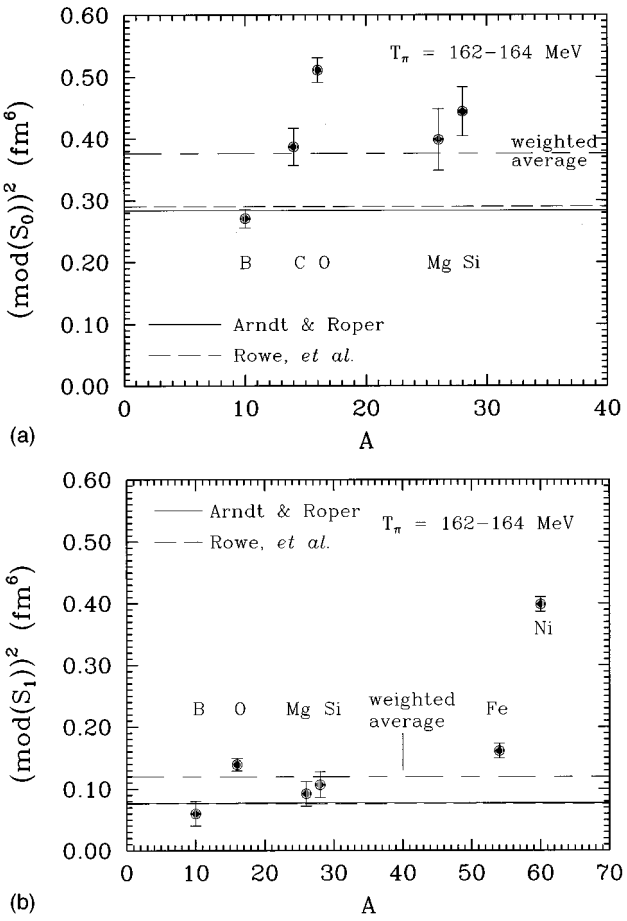

FIG. 4. Empirical measurements of and phase-shift predictions for the isoscalar (a) and isovector (b) spin-flip strength parameters for the resonance energy data discussed in the text. The phase shift predictions of Arndt and Roper [3] and Rowe, Salomon, and Landau [4] are indicated by the solid and dashed lines, respectively. Long-short-dashed lines in (a) and (b) represent the weighted average of the empirical measurement. The weighted average of the $|S_1|^2$ data does not include the nickel or iron data.

The empirical strength parameters at resonance determined in this analysis for the ^{10}B, ^{16}O, and ^{28}Si nuclei are larger in magnitude than those determined previously using MSU potential parameters [15,18]. The enhancement appears to be the same for the three nuclei, however. A weighted average of the empirical $|S_0|^2$ and $|S_1|^2$ values obtained at 162 MeV for the specified nuclei gives values of (0.376 ± 0.010) fm^6 for the isoscalar strength and (0.189 ± 0.005) fm^6 for the isovector strength.

As at 65 MeV, these empirical values of the strength parameters differ from the values using the phase shifts of Arndt and Roper [3]. The weighted average value for the enhancement of the isovector strength at 162 MeV was

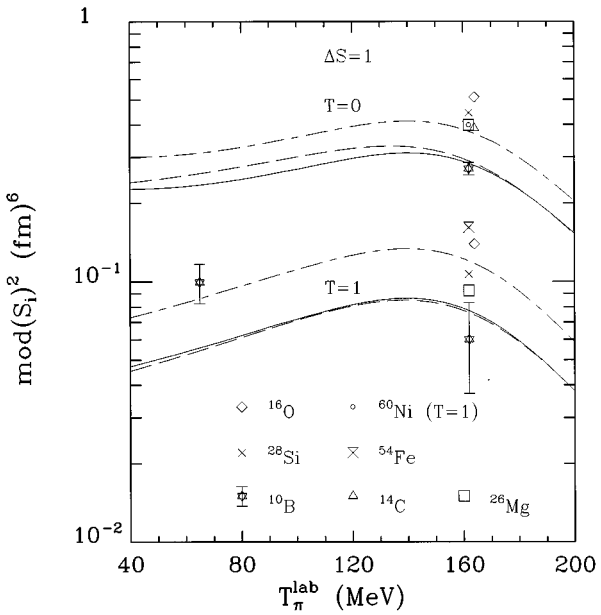

FIG. 5. Comparisons of the target independent strength parameter using the phase shifts of Arndt and Roper (solid lines) and Rowe, Salomon, and Landau (dashed lines) [3,4]. The long-short-dashed lines are given by the weighted average of the empirically determined values for the resonance energy data. The nickel data point shown is for an isovector transition, though it overlaps isoscalar data for other data. The weighted average for the $T=1$ data does not include the ^{54}Fe and ^{60}Ni data.

found to be 2.45 ± 0.06, while that for the isoscalar strength was found to be 1.33 ± 0.03. The resulting predictions are illustrated as the solid lines in Figs. 4(a), 4(b), and 5.

The large value inferred for the enhancement of the isovector strength at resonance is due mostly to the large normalization needed to make the predicted cross sections for ^{60}Ni agree with the data. If one were to examine the lighter nuclei, without including the ^{54}Fe and ^{60}Ni data in the computation of the isovector strength, the enhancement factor needed would be 1.55 ± 0.09 and the weighted average value would be 0.12 ± 0.01. The error associated with the strength parameter is again related to the uncertainties of the measured cross sections and statistical variations. Curves representing these two enhancements without inclusion of the ^{54}Fe and ^{60}Ni data are shown as the long-short dashed curves in Figs. 4(a), 4(b), and 5.

Hence, *at both 65 MeV and at resonance energies, the empirically measured spin-flip strength is enhanced over the value expected from phase shifts.*

D. Energy dependence of isovector spin-flip strength

Combining the results of the analyses at resonance and at 65 MeV provides the first determination of the energy dependence of isovector strength parameter, as is illustrated in Fig. 5, where some of the error bars are omitted for clarity. The isovector strength enhancement at 65 MeV is consistent with the weighted average enhancement observed at resonance when the ^{54}Fe and ^{60}Ni data are excluded from the average. Though more data would be useful, the data shown in Fig. 5 suggest that the energy dependence of the isovector strength enhancement is small or nonexistent.

Results for the isovector strength using different phase shifts are illustrated by a comparison, shown in Figs. 4(a), 4(b), and 5, of the predictions using the phase shift analyses of Arndt and Roper [3] and those of Rowe, Salomon, and Landau [4]. No significant difference based on the choice between these two phase shift analyses is observed for the isovector spin-flip strength. A similar analysis shows some dependence on the choice of phase shifts for the isoscalar predictions, as is also shown in Figs. 4(a), 4(b), and 5.

This reaction mechanism formalism assumes that the strength parameters do not include any variation with target mass. Examination of the data in Figs. 4(a) and 4(b) suggests that the strength parameters may in fact have some weak dependence on target mass since, when the nickel data are not included, the trend of the strength parameters suggests a dependence on A. This enhancement, since it, at least initially, grows with A, may be attributable to a mass density effect, since an increasing portion of the nucleus is at central density as the mass increases.

IV. CONCLUSIONS

In conclusion, these measurements of low energy pion scattering have permitted the determination of the energy dependence of the isovector portion of the strength parameter for the pion-nucleus interaction. A consistent enhancement of the empirical isovector strength parameter by a factor of about 1.7 over that obtained from phase shifts is observed at both energies studied, suggesting that the energy dependence is small or nonexistent. At resonance, the empirical isoscalar strength is enhanced by a factor of about 1.3. A slight mass dependence in both of these enhancement factors is also suggested.

ACKNOWLEDGMENTS

We gratefully acknowledge helpful discussions with J. A. Carr, W. B. Kaufmann, and R. J. Peterson. This work was supported by the National Science Foundation and the U.S. Department of Energy.

[1] J. A. Carr, F. Petrovich, D. Halderson, D. B. Holtkamp, and W. B. Cottingame, Phys. Rev. C **27**, 1636 (1983).

[2] T. Suzuki, S. Krewald, and J. Speth, Phys. Lett. **107B**, 9 (1981).

[3] R. A. Arndt and L. O. Roper, program SAID (Scattering Analysis Interactive Dial-In), SM95.

[4] G. Rowe, M. Salomon, and R. H. Landau, Phys. Rev. C **18**, 584 (1978).

[5] F. Ajzenberg-Selove, Nucl. Phys. **A490**, 1 (1988).

[6] B. Zeidman *et al.*, Phys. Rev. C **38**, 2251 (1988).

[7] R. L. Burman, R. Fulton, and M. Jakobson, Nucl. Instrum. Methods **131**, 29 (1975).

[8] J. D. Zumbro, H. A. Thiessen, C. L. Morris, and J. A. McGill, Nucl. Instrum. Methods Phys. Res. B **40/41**, 896 (1989).
[9] J. M. O'Donnell, *et al.*, Nucl. Instrum. Methods Phys. Res. A **314**, 409 (1992).
[10] J. M. O'Donnell *et al.*, Nucl. Instrum. Methods Phys. Res. A **317**, 445 (1992).
[11] J. Mitchell, Ph.D. thesis, University of Colorado, Los Alamos Report No. LA-10941-T.
[12] J. M. Applegate, M.S. thesis, Arizona State University, Los Alamos Report No. LA-12487-T.
[13] M. Blecher *et al.*, Phys. Rev. C **28**, 2033 (1983).
[14] C. L. Morris, NEWFIT curve fitting program, LAMPF software, 1990, unpublished.
[15] J. A. Carr, F. Petrovich, D. Halderson, and J. Kelly, scattering potential code ALLWRLD, unpublished.
[16] J. A. Carr, 1985 version of the computer program MSUDWPI, unpublished; adapted from the computer program DWPI, R. A. Eisenstein and G. A. Miller, Comput. Phys. Commun. **11**, 95 (1976).
[17] J. A. Carr, H. McManus, and K. Stricker-Bauer, Phys. Rev. C **25**, 952 (1982).
[18] B. L. Clausen *et al.*, Phys. Rev. C **41**, 2246 (1990).
[19] B. L. Clausen *et al.*, Phys. Rev. C **48**, 1632 (1993).
[20] J. A. Carr, private communication.
[21] H. De Vries, C. W. De Jager, and C. De Vries, At. Data Nucl. Data Tables **36**, 495 (1987).
[22] E. J. Ansaldo, J. C. Bergstrom, R. Yen, and H. S. Caplan, Nucl. Phys. **A322**, 237 (1979).
[23] P. R. Lewis *et al.*, Nucl. Phys. **A532**, 583 (1991).
[24] T.-S. H. Lee and D. Kurath, Phys. Rev. C **21**, 293 (1980).
[25] T. Sato, N. Odagawa, H. Ohtsubo, and T.-S. H. Lee, Phys. Rev. C **49**, 776 (1994).
[26] J. C. Bergstrom, private communication.
[27] C. Olmer *et al.*, Phys. Rev. Lett. **43**, 612 (1979).
[28] D. B. Holtkamp *et al.*, Phys. Rev. Lett. **45**, 420 (1980).
[29] D. B. Holtkamp *et al.*, Phys. Rev. C **31**, 957 (1985).
[30] D. F. Geesaman *et al.*, Phys. Rev. C **30**, 952 (1984).
[31] J. Piffaretti *et al.*, Phys. Lett. **71B**, 324 (1977).
[32] S. J. Seestrom-Morris, Ph.D. thesis, University of Minnesota, Los Alamos Report No. LA-8916-T.
[33] B. Zeidman *et al.*, Phys. Rev. Lett. **40**, 1539 (1978).
[34] Q. Ingram *et al.*, Phys. Lett. **76B**, 173 (1978).